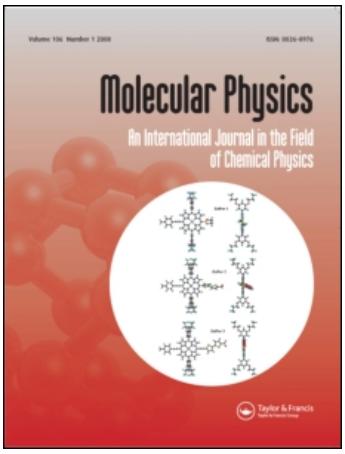

Molecular Physics
Publication details, including instructions for authors and subscription information:
http://www.informaworld.com/smpp/title~content=t713395160

Spatial correlation of dipole fluctuations in liquid water

M. J. McGrath [a]; J. I. Siepmann [a]; I.-F. W. Kuo [b]; C. J. Mundy [c]
[a] Departments of Chemistry and of Chemical Engineering and Material Science, University of Minnesota, Minneapolis, Minnesota 55455, USA [b] Chemistry, Materials and Science Directorate, Lawrence Livermore Chemistry, National Laboratory, Livermore, California 94550, USA [c] Chemistry and Materials Science Division, Pacific Northwest National Laboratory, Richland, WA 99352, USA

Online Publication Date: 01 May 2007

To cite this Article McGrath, M. J., Siepmann, J. I., Kuo, I.-F. W. and Mundy, C. J.(2007)'Spatial correlation of dipole fluctuations in liquid water',Molecular Physics,105:10,1411 — 1417
To link to this Article: DOI: 10.1080/00268970701364938
URL: http://dx.doi.org/10.1080/00268970701364938

Molecular Physics, Vol. 105, No. 10, 20 May 2007, 1411–1417

Taylor & Francis
Taylor & Francis Group

Spatial correlation of dipole fluctuations in liquid water

M. J. MCGRATH†, J. I. SIEPMANN*†, I.-F. W. KUO‡, C. J. MUNDY§

†Departments of Chemistry and of Chemical Engineering and Material Science, University of Minnesota, 207 Pleasant St. SE, Minneapolis, Minnesota 55455, USA
‡Chemistry, Materials and Science Directorate, Lawrence Livermore National Laboratory, Livermore, California 94550, USA
§Chemistry and Materials Science Division, Pacific Northwest National Laboratory, Richland, WA 99352, USA

(*Received 27 February 2007; in final form 23 March 2007*)

The molecular dipole moments and local environments of water in its liquid phase were examined for a series of first-principles Gibbs ensemble Monte Carlo simulations along the vapour–liquid coexistence curve using the Becke–Lee–Yang–Parr (BLYP) and Perdew–Burke–Ernzerhof (PBE) exchange/correlation density functionals. Molecular dipole moments were computed using maximally localized Wannier functions with the Berry phase scheme, while the structure was analysed with respect to tetrahedral order parameter and hydrogen bonding. Increasing the temperature results in a decrease of both the average molecular dipole moment and the local structure, although the width of the dipole distribution remains fairly constant. A correlation is found between the extent of the local structure and the magnitude of the molecular dipole moment, but this correlation is limited to the first solvation shell.

1. Introduction

Water is the most important solvent on earth, largely due to its high dipole moment and polarizability. Despite years of research, a complete understanding of water does not exist today [1–3]. The dipole moment of an isolated water molecule in the gas phase has been well established to be 1.85 D [4]. Chemical intuition suggests that the dipole moment of a water molecule will increase when placed in its liquid phase due to polarization effects, but the extent of this increase and the width of the dipole moment distribution has not yet been determined. Many efforts have been made to determine these quantities, including extrapolations from small clusters [5, 6], chemical theory [7–10], empirical polarizable models [11–18], semi-empirical methods [19], combined quantum mechanical/molecular mechanical (QM/MM) methods [20–26], fully quantum mechanical methods with a single molecule in strong electric fields [27–29], and first-principles molecular simulation [30–42]. While the full range of values shows significant spread, it is commonly accepted that the liquid phase dipole moment of water falls between 2.5–3.0 D. The most recent experimental result is 2.95 ± 0.6 D [43]. It should be noted that widely-used, fixed-charge models for water generally possess smaller dipole moments (e.g. 2.35 D for SPC/E [44], 2.45 D for TIP3P [45] and 2.18 D for TIP4P [45]).

The use of molecular simulation to explore the electronic structure of water has several strengths, in particular the ability to probe experimentally accessible state points and to analyse microscopic structure. Explicit simulation also provides the ability to treat the whole system at the same level of theory. Since the first simulations of liquid water using empirical force fields [46, 47], methods and interaction potentials have advanced dramatically. Despite these advances, however, empirical models still struggle to reproduce thermophysical properties of water in varied environments and for different state points [3]. The advent of the Car–Parrinello (CP) method in 1985 [48] enabled researchers to run molecular simulations with interaction potentials described by Kohn–Sham (KS) density functional theory [49], which, in principle, should be completely transferable and robust.

While the bulk of previous investigations of the dipole moment of liquid water using first-principles molecular simulations have been limited to ambient conditions, some work has also been done on supercritical water at elevated temperature and reduced density [34, 35, 40]. The overwhelming majority of previous first-principles

*Corresponding author. Email: siepmann@chem.umn.edu

Molecular Physics
ISSN 0026–8976 print/ISSN 1362–3028 online
http://www.tandf.co.uk/journals
DOI: 10.1080/00268970701364938

molecular simulations (with the exception of [37, 38, 41, 42]) were performed at constant density. To our knowledge, only one work has reported on the temperature dependence of the molecular dipole moments of liquid water along the coexistence curve using first-principles interaction potentials [41]. Here we present a more in-depth analysis of the temperature and structural dependence of the molecular dipole moment of the liquid phase of water described by Kohn–Sham density functional theory using two different functionals.

2. Computational details

Monte Carlo (MC) simulations were performed in the Gibbs ensemble [50, 51] as implemented in the CP2K package (http://cp2k.berlios.de). The systems are described by Kohn–Sham density functional theory [49] with the energies computed by the Quickstep subroutines [52], which solve the self-consistent Kohn–Sham equations using an atom-centred Gaussian-type basis set for the molecular orbitals and an auxiliary plane-wave basis set to expand the electronic density [53]. Simulations were run for a total of 64 molecules for the Becke–Lee–Yang–Parr (BLYP) [54, 55] exchange/correlation density functional at $T = 323$, 423 and 523 K, while simulations for the Perdew–Burke–Ernzerhof (PBE) [56] functional were performed at $T = 423$, 523 and 623 K, due to its significantly higher critical temperature. A triple-ζ basis set with two sets of p-type or d-type polarization functions (TZV2P) has been previously shown to be appropriate for calculations involving functionals with the generalized gradient approximation (GGA) [52, 57]. The norm-conserving pseudopotentials of Goedecker, Teter and Hutter (GTH) [58, 59] were used to mimic core electrons. A plane-wave cutoff of 1200 Ry is required to converge system energies in some simulations involving fluctuating cell volumes [38]. The complete simulation details are given elsewhere [41, 42].

All analysis presented here was done on a total of 200 configurations per run, taken from the last 200 cycles of each simulation after the system had equilibrated. The molecular dipole moments were computed from maximally localized Wannier functions with the Berry phase scheme [31, 60, 61]. As a measure of the structure of the local water environment we use the tetrahedral order parameter (q) as renormalized by Errington and Debenedetti [62]. The value of q will be unity for a water molecule with four neighbours creating a perfect tetrahedron and zero for the ensemble average of a completely disordered system. The combined distance–angular criterion proposed by Wernet *et al.* [63] is used to determine whether a hydrogen bond is formed between two molecules.

3. Results and discussion

Figure 1 shows representative configurations of all six simulations with the molecules coloured according to their dipole moment, while figure 2 shows the distribution of molecular dipole moments throughout the simulations. As already noted in [41], the magnitude of the dipole moment varies greatly even in a single configuration and the average dipole moment in the saturated liquid phase changes significantly with the temperature (see also table 1). It is clear that the highest temperature for both BLYP and PBE have very few molecules with a large dipole moment ($\langle\mu\rangle > 3.0$). This is expected for two reasons: (1) the density at these temperatures is relatively low and (2) thermal energy allows the molecules to venture away from orientations that induce high dipole moments. For opposite reasons, BLYP-GTH-TZV2P-1200 at $T = 323$ K contains the highest concentration of molecules with large dipole moments. One interesting feature of figures 1 and 2 is the similarity of the two low temperatures for the PBE simulations when compared to the two lowest temperature BLYP runs. This can be explained when one takes the average density of the simulations into account: the average densities of the two coolest PBE runs differ by only 3% while the BLYP densities are different by 20% [42], resulting in less variation of the intermolecular distances and more similar induction effects for PBE. It should be noted here that this very large decrease in density found for BLYP is at least in part related to the large uncertainties in first principles Gibbs ensemble simulations because the density scaling law requires that the magnitude of the slope of ρ_{liq} versus T should decrease with increasing T, which is not observed for the three BLYP simulations in [41].

The average values of several observables from the simulations and a measure of the spread of their instantaneous distributions are given in table 1. In addition to the molecular dipole moment, a measure of local structure is also included. This quantity, q, is called the tetrahedral order parameter and signifies the extent of tetrahedral ordering around a given molecule [62]. One expected result shown in this table is the systematic decrease of both the average μ and q as the temperature increases. This is due in part to the corresponding decrease in density and partly due to the disruption of the hydrogen bond network as molecules gain enough thermal energy to sample energetically less favourable configurations. Table 1 also suggests that

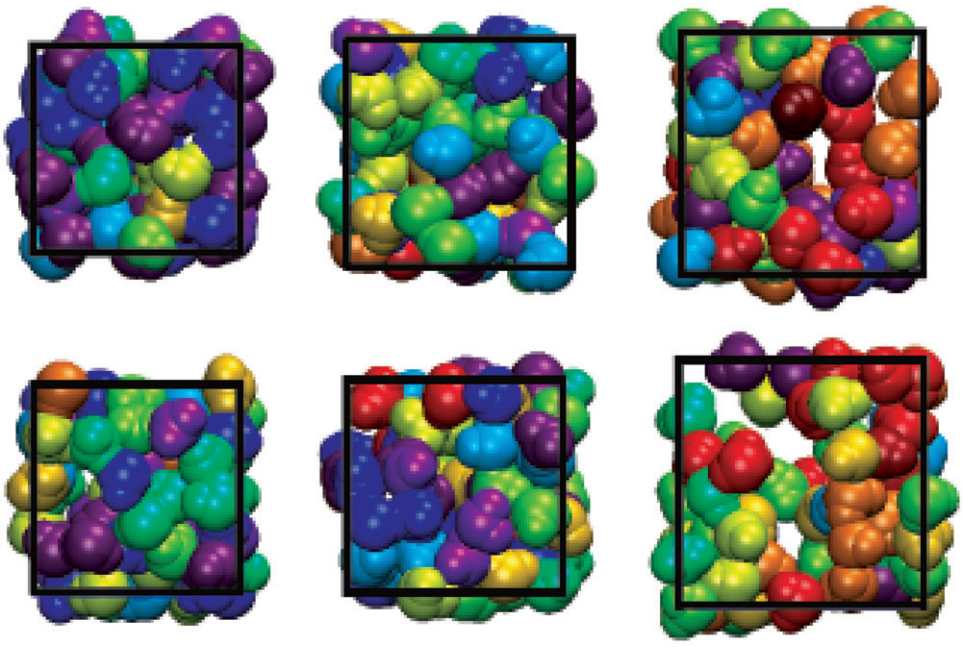

Figure 1. Snapshots of the liquid phase taken from Gibbs ensemble Monte Carlo simulations of water. The top panel depicts BLYP-GTH-TZV2P-1200 at $T = 323$, 423 and 523 K (from left to right) and the bottom panel shows PBE-GTH-TZV2P-1200 at $T = 423$, 523 and 623 K (from left to right). The molecules are coloured according to their instantaneous molecular dipole moment (μ). The visible spectrum was evenly partitioned to represent dipole magnitudes of 1.9–3.2 D in increments of 0.1 D, with red indicating low values.

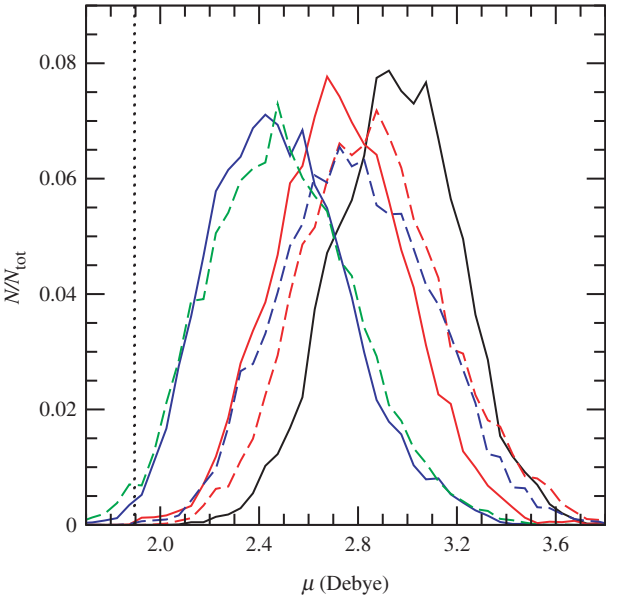

Figure 2. The fraction of molecules with a given instantaneous molecular dipole moment for all simulations reported in this work. BLYP and PBE are depicted by solid and dashed lines, respectively. Black, red, blue and green lines represent $T = 323$, 423, 523 and 623 K, respectively. The bin width for the distributions is 0.05 D. The vertical dotted line is the value of the dipole moment for an isolated water molecule (BLYP and PBE give an identical result out to three significant figures).

Table 1. Average values of the saturated liquid density (ρ_{liq}), molecular dipole moment (μ) and tetrahedral order parameter (q) for all six runs investigated in this work. Numbers in parenthesis are the full width at half maximum (FWHM) of Gaussian functions fit to the distributions of the instantaneous values. The full distributions for μ and q are shown in figures 2 and 3. An estimation is used for q, as the peaks are not symmetrical due to the order parameter having a maximum value.

Functional	T (K)	$\langle\rho_{liq}\rangle$ (g cm^{-3})	$\langle\mu\rangle$ (Debye)	$\langle q\rangle$
BLYP	323	0.89 (0.03)[a]	2.96 (0.60)	0.73 (0.4)
BLYP	423	0.71 (0.06)[a]	2.73 (0.63)	0.55 (0.6)
BLYP	523	0.56 (0.15)[a]	2.49 (0.65)	0.41 (0.5)
PBE	423	0.88 (0.06)[b]	2.87 (0.67)	0.58 (0.6)
PBE	523	0.85 (0.06)[b]	2.80 (0.73)	0.55 (0.5)
PBE	623	0.57 (0.10)[b]	2.49 (0.70)	0.35 (0.5)

[a]From [41].
[b]From [42].

BLYP and PBE will have an average molecular dipole moment around 3.0 D at ambient conditions, a suggestion that is also supported by both fixed-density [31, 40] and interfacial simulations [37].

The simulations in the literature that correspond closest to the temperatures and densities shown here were performed on supercritical water using the BLYP

functional at $\rho = 0.73\,\mathrm{g\,cm^{-3}}$ and $T = 653\,\mathrm{K}$, and give an average dipole moment of $2.35 \pm 0.38\,\mathrm{D}$ [34]. Other results for the BLYP functional at $\rho = 0.6\,\mathrm{g\,cm^{-3}}$ and $T = 700\,\mathrm{K}$ show an average dipole moment of $2.15 \pm 0.27\,\mathrm{D}$, but these values were computed using the atoms-in-molecules approach of Bader [64] and result in systematically lower values than the Wannier centre method [40]. Compared to our simulations for the saturated liquid phase, the simulations of [34] make it appear that the dipole moment depends more strongly on temperature than on density, i.e. our simulations for BLYP at 523 K (a 20% reduction in temperature and 23% in density compared to the simulations of Boero *et al.* [34]) show more enhanced dipole moments. Consequently, it may be more instructive to compare to the PBE simulations reported here at $T = 623\,\mathrm{K}$, which show a slightly higher average μ at a much lower density (it is important to remember that Boero *et al.* used the BLYP functional, so direct comparisons are difficult). Dyer and Cummings found that the average liquid dipole moment of BLYP water drops by about 0.25 D with a temperature increase of 200 K (from 300 to 500 K) at fixed density [40]. The average molecular dipole difference for that same temperature range and functional reported here is 0.47 D, suggesting that the temperature and density effects may be comparable (if the same 60% temperature increase accounts for 0.25 D difference, then the remaining 0.22 D difference is the effect of the 40% density decrease). Therefore, the dominating cause of the dipole change remains ambiguous. Finally, it should be noted that the width of the distribution appears to be around 0.6 D [40] to 0.7 D [34] in supercritical water, which again is similar to the spread of values shown here at high temperatures.

Figure 3 is a plot of the distribution of the tetrahedral order parameter for the six simulations. From this we can see that only the BLYP simulation at 323 K is anywhere near a highly ordered system. One may have expected PBE at 423 K to show a similar degree of ordering because it falls near the same reduced temperature (T/T_c), but this does not appear to be the case. Another feature is the broadness of the distributions. Given that the average value of q falls between 0.35 and 0.73, the full width at half maximum (FWHM) of about 0.5 is of similar magnitude. However, while the tails of the distributions shown in figure 3 extend beyond 0, the average values are still larger than 0, indicating that the system is reasonably far from showing uniform orientational distributions. This view is supported by the distribution of dipole moments in figure 2, the instantaneous snapshots in figure 1, and that the average μ is at least 0.6 D greater than that of an isolated water molecule.

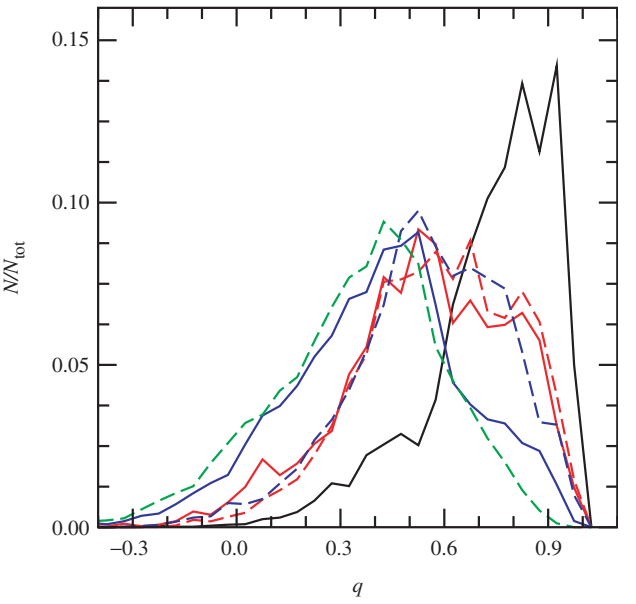

Figure 3. The fraction of the number of molecules with a given instantaneous tetrahedral order parameter as renormalized by Errington and Debenedetti [62]. The line styles are the same as in figure 2. The bin width is 0.05 units.

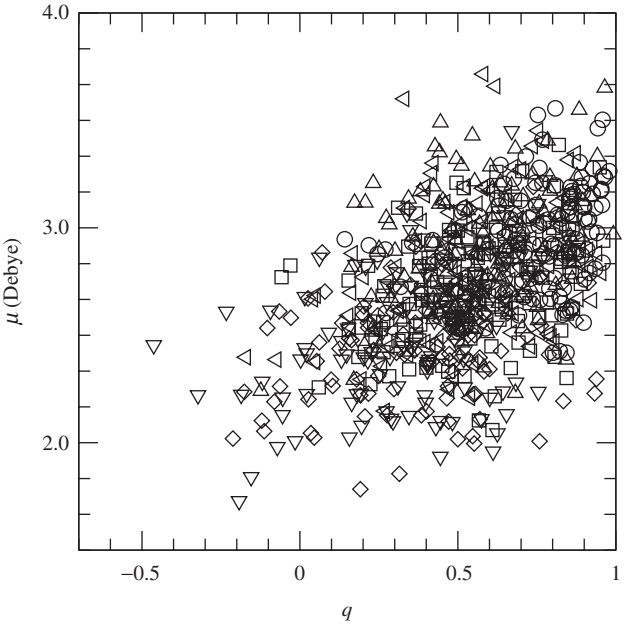

Figure 4. A plot of the instantaneous molecular dipole moment as a function of the tetrahedral order parameter for all simulations. Circles, squares and diamonds represent BLYP-GTH-TZV2P-1200 at $T = 323$, 423 and 523 K, respectively, while triangles up, left and down depict PBE-GTH-TZV2P-1200 at $T = 423$, 523 and 623 K. Only every 100th symbol is shown for clarity.

It remains instructive to examine the relationship between the local structure of a water molecule and its dipole moment. As can be seen in figure 4, some correlation exists, as the distribution takes the

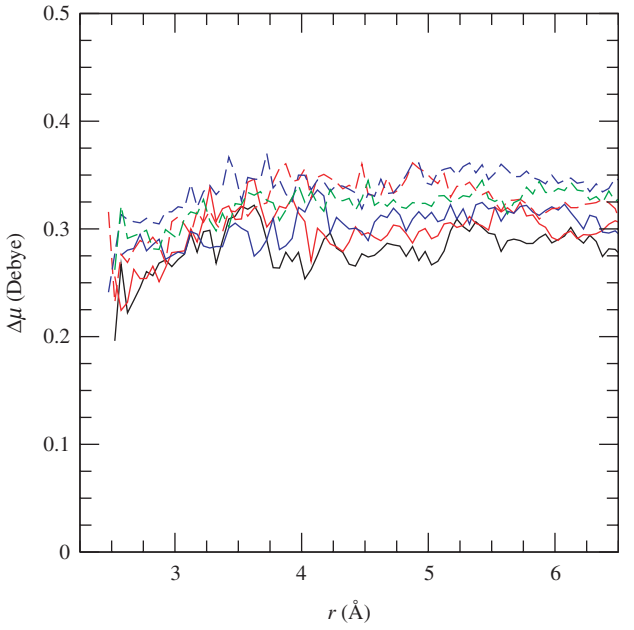

Figure 5. The average difference in molecular dipole moment as a function of oxygen–oxygen distance. Points are only shown for bins with more than 100 pairs. The line styles are the same as figure 2. The bin size is 0.05 Å.

shape of an ellipse with a positive slope for the line connecting the foci. A linear fit yields a slope of 0.62μ and a correlation coefficient of 0.49. It is not expected that there would exist a perfect correlation between the two values as the order parameter is based solely on the oxygen positions and neglects the relative orientation of the dipole vectors of the molecules, while the induced dipole moment depends on this orientation. Consequently, one can conclude that there does exist some relationship between the local tetrahedral structure and the induced molecular dipole moment.

The induced dipole–dipole interaction is known to fall off rapidly with distance (r^{-6}) [65], and therefore it is not expected that the induced dipole of one water molecule will directly affect other molecules outside the first or second solvation shell. Figure 5 shows how the dipole difference between two molecules depends weakly on the oxygen–oxygen distance. It can be seen from this figure that all simulations level off at a value very close to 0.5 FWHM (see table 1). The lines appear to have a positive slope for $r_{OO} < 4$ Å, indicating that the spread of dipole moments decreases as the distance between the two molecules decreases. It is also very clear that this effect does not extend beyond the first solvation shell, and it is not very strong (the difference reduces by 0.05 D at most).

Table 2 extends the exploration of the relationship between dipole moment and local structure. Based on the combined distance–angular bonding criteria set forth by Wernet *et al.* [63] one can classify a water molecule according to the number and type of hydrogen bonds it forms with neighbours. This table shows that molecules experiencing more hydrogen bonding have on average higher dipole moments, which is understandable as by its nature, a hydrogen bond will form between a hydrogen with a partial positive charge and an oxygen with a partial negative charge, which is an orientation that enhances the induced dipole moment. Because none of the similar sites are symmetric through the centre of the molecule, the effects will not cancel each other out. The dipole moment for molecules with fully saturated hydrogen bonding (double acceptor/double donor; DA/DD) is about 30% larger than those not forming a hydrogen bond (non-acceptor/non-donor; NA/ND). While the data for only two simulations is shown in table 2, similar values are found in all runs. Additional analysis reveals that the dipole difference between molecules which share a hydrogen bond is 0.28 D. This value is slightly below the average long-range value seen in figure 5, again showing that there is a small increase in dipole correlation between molecules in the first solvation shell.

Table 2. Average values of $\mu/\bar{\mu}$ for a given characterization of water. ND, SD, DD, NA, SA and DA signify non-donor, single-donor, double–donor, non-acceptor, single-acceptor and double-acceptor molecules, respectively, according to the criterion suggested by Wernet *et al.* [63]. Data is shown for the intermediate temperature for both functionals ($T = 423$ K for BLYP and $T = 523$ K for PBE).

	BLYP			PBE		
	ND	SD	DD	ND	SD	DD
NA	0.84	0.93	1.00	0.84	0.92	0.98
SA	0.92	1.00	1.04	0.90	0.98	1.04
DA	0.95	1.04	1.09	0.96	1.02	1.08

Figure 6 shows the distribution of the molecular dipole moment for the two simulations shown in table 2 as a function of the total number of hydrogen bonds the molecule is involved in. Unlike table 2, figure 6 does not distinguish between donors and acceptors (i.e. SA/SD is classified in the same manner as DA/ND because they both have a total of two hydrogen bonds). The effect of the number of hydrogen bonds on the dipole moment is clear, as the distributions for zero hydrogen bonds and four hydrogen bonds show minimal overlap; both of these distributions show considerable overlap with that of an intermediate number of hydrogen bonds. These results appear to be independent of the choice of functional and agree well with the trends shown in table 2.

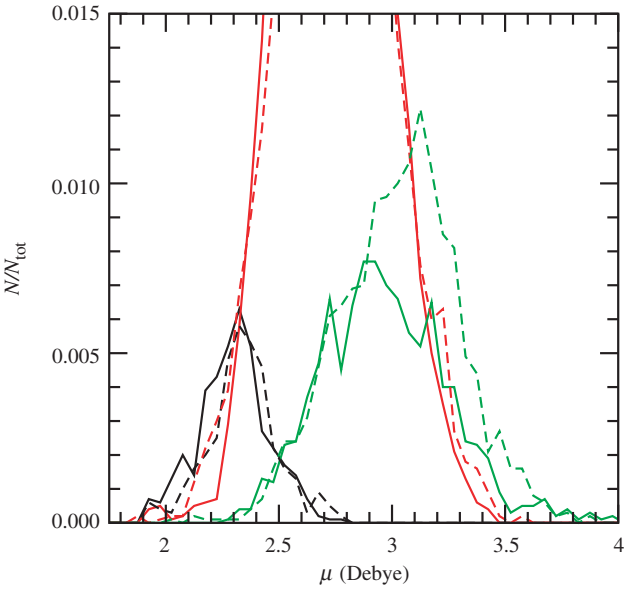

Figure 6. The distribution of the molecular dipole moment as a function of the number of hydrogen bonds a molecule is engaged in (as either a donor or acceptor). Black represents no hydrogen bonds, red is for two hydrogen bonds, and green is for four hydrogen bonds. The solid and dashed lines depict the results for BLYP ($T = 423$ K) and PBE ($T = 523$ K), respectively. The bin size is 0.05 D.

4. Conclusion

An analysis of the molecular dipole moments and structural features obtained from first principles Gibbs ensemble Monte Carlo simulations of water shows that the average liquid-phase dipole moment decreases with increasing temperature (and correspondingly decreasing saturated density). Comparison to simulations for supercritical water [34, 35, 40] indicates that temperature and density play approximately equal roles in determining the average molecular dipole moment. In agreement with other first principles simulations [31, 34, 37, 40] we find that the width of the dipole moment distribution is not extremely sensitive to changes in temperature and density. Our simulations reveal a correlation between the local tetrahedral order and the dipole moment of a given molecule with a slope of about 0.6μ but a correlation coefficient of only about 0.5. In general, molecules involved in more hydrogen bonds possess higher dipole moments. Furthermore, dipole moments of two molecules that belong to each others' first solvation shell possess dipole moments only slightly more correlated than for more distant molecules. It appears that the number of hydrogen bonds a molecule is involved in correlates more with the magnitude of the molecular dipole moment than the tetrahedral order parameter, a conclusion justified by the tetrahedral order parameter being solely a function of oxygen position while the hydrogen bond criterion used here includes an orientational dependence.

Acknowledgements

We thank Larry Fried and Charlie Westbrook for their ongoing support of this work. We also thank Juerg Hutter, Joost VandeVondele and Matthias Krack for many stimulating discussions. Financial support from the National Science Foundation (CTS-0553911), a 3M Foundation Graduate Fellowship (MJM), and a Department of Energy Computational Science Graduate Fellowship (MJM) are gratefully acknowledged. Part of this work was performed under the auspices of the US Department of Energy by the University of California Lawrence Livermore National Laboratory (LLNL) under contract No. W-7405-Eng-48. Computer resources were provided by Livermore Computing and the Minnesota Supercomputing Institute.

References

[1] F. H. Stillinger, Science **209,** 451 (1980).
[2] J. P. Hansen and I. R. McDonald, *Theory of Simple Liquids*, 3rd ed. (Academic Press, New York, 2006).
[3] B. Guillot, J. Molec. Liq. **101,** 219 (2002).
[4] S. A. Clough, Y. Beers, G. P. Klein, and L. S. Rothman, J. Chem. Phys. **59,** 2254 (1973).
[5] J. K. Gregory, D. C. Clary, K. Liu, M. G. Brown, and R. J. Saykally, Science **275,** 814 (1997).
[6] Y. Tu and A. Laaksonen, Chem. Phys. Lett. **329,** 283 (2000).
[7] L. Onsager, J. Am. Chem. Soc. **58,** 1486 (1936).
[8] J. G. Kirkwood, J. Chem. Phys. **7,** 911 (1939).
[9] C. A. Coulson and D. Eisenberg, Proc. R. Soc. A **291,** 445 (1966).
[10] A. P. Minton, Chem. Phys. Lett. **7,** 606 (1970).
[11] M. Sprik, J. Chem. Phys. **95,** 6762 (1991).
[12] S. W. Rick, S. J. Stuart, and B. J. Berne, J. Chem. Phys. **101,** 6141 (1994).
[13] L. X. Dang and T.-M. Chang, J. Chem. Phys. **106,** 8149 (1997).
[14] B. Chen, J. Xing, and J. I. Siepmann, J. Phys. Chem. B **104,** 2391 (2000).
[15] Y. Wu and Z.-Z. Yang, J. Phys. Chem. A **108,** 7563 (2004).
[16] P. Paricaud, M. Předota, A. A. Chialvo, and P. T. Cummings, J. Chem. Phys. **122,** 244511 (2005).
[17] N. J. English, Molec. Phys. **103,** 1945 (2005).
[18] I.-F. W. Kuo, C. J. Mundy, B. L. Eggimann, M. J. McGrath, J. I. Siepmann, B. Chen, J. Vieceli, and D. J. Tobias, J. Phys. Chem. B **110,** 3738 (2006).
[19] G. Monard, M. I. Bernal-Uruchurtu, A. van der Vaart, K. M. Merz Jr, and M. F. Ruiz-López, J. Phys. Chem. A **109,** 3425 (2005).

[20] J. Bertran, M. F. Ruiz-López, D. Rinaldi, and J. L. Rivail, Theo. Chim. Acta **84,** 181 (1992).
[21] J. Gao, F. J. Luque, and M. Orozco, J. Chem. Phys. **98,** 2975 (1993).
[22] S. Chalmet and M. F. Ruiz-López, J. Chem. Phys. **115,** 5220 (2001).
[23] J. Kongsted, A. Osted, K. V. Mikkelsen, and O. Christiansen, Chem. Phys. Lett. **364,** 379 (2002).
[24] T. D. Poulsen, P. R. Ogilby, and K. V. Mikkelsen, J. Chem. Phys. **116,** 3730 (2002).
[25] Y. Tu and A. Laaksonen, Int. J. Quantum Chem. **102,** 888 (2005).
[26] A. Osted, J. Kongsted, K. V. Mikkelsen, P.-O. Åstrand, and O. Christiansen, J. Chem. Phys. **124,** 124503 (2006).
[27] A. V. Gubskaya and P. G. Kusalik, Molec. Phys. **99,** 1107 (2001).
[28] A. V. Gubskaya and P. G. Kusalik, J. Chem. Phys. **117,** 5290 (2002).
[29] K. Coutinho, R. C. Guedes, B. J. Costa Cabral, and S. Canuto, Chem. Phys. Lett. **369,** 345 (2003).
[30] K. Laasonen, M. Sprik, M. Parrinello, and R. Car, J. Chem. Phys. **99,** 9080 (1993).
[31] P. L. Silvestrelli and M. Parrinello, Phys. Rev. Lett. **82,** 3308 (1999).
[32] P. L. Silvestrelli and M. Parrinello, J. Chem. Phys. **111,** 3572 (1999).
[33] L. Delle Site, A. Alavi, and R. M. Lynden-Bell, Molec. Phys. **96,** 1683 (1999).
[34] M. Boero, K. Terakura, T. Ikeshoji, C. C. Liew, and M. Parrinello, Phys. Rev. Lett. **85,** 3245 (2000).
[35] M. Boero, K. Terakura, T. Ikeshoji, C. C. Liew, and M. Parrinello, J. Chem. Phys. **115,** 2219 (2001).
[36] A. Pasquarello and R. Resta, Phys. Rev. B **68,** 174302 (2003).
[37] I.-F. W. Kuo and C. J. Mundy, Science **303,** 658 (2004).
[38] M. J. McGrath, J. I. Siepmann, I.-F. W. Kuo, C. J. Mundy, J. VandeVondele, J. Hutter, F. Mohamed, and M. Krack, Chem. Phys. Chem. **6,** 1894 (2005).
[39] T. Todorova, A. P. Seitsonen, J. Hutter, I.-F. W. Kuo, and C. J. Mundy, J. Phys. Chem. B **110,** 3685 (2006).
[40] P. J. Dyer and P. T. Cummings, J. Chem. Phys. **125,** 144519 (2006).
[41] M. J. McGrath, J. I. Siepmann, I.-F. W. Kuo, C. J. Mundy, J. VandeVondele, J. Hutter, F. Mohamed, and M. Krack, J. Phys. Chem. A **110,** 640 (2006).
[42] M. J. McGrath, J. I. Siepmann, I.-F. W. Kuo, and C. J. Mundy, Molec. Phys. **104,** 3619 (2006).
[43] Y. S. Badyal, M.-L. Saboungi, D. L. Price, S. D. Shastri, D. R. Haeffner, and A. K. Soper, J. Chem. Phys. **112,** 9206 (2000).
[44] H. J. C. Berendsen, J. R. Grigera, and T. P. Straatsma, J. Phys. Chem. **91,** 6269 (1987).
[45] W. L. Jorgensen, J. Chandrasekhar, J. D. Madura, R. W. Impey, and M. L. Klein, J. Chem. Phys. **79,** 926 (1983).
[46] J. A. Barker and R. O. Watts, Chem. Phys. Lett. **3,** 144 (1969).
[47] A. Rahman and F. H. Stillinger, J. Chem. Phys. **55,** 3336 (1971).
[48] R. Car and M. Parrinello, Phys. Rev. Lett. **55,** 2471 (1985).
[49] W. Kohn and L. J. Sham, Phys. Rev. **140,** A1133 (1965).
[50] A. Z. Panagiotopoulos, Molec. Phys. **61,** 813 (1987).
[51] A. Z. Panagiotopoulos, N. Quirke, M. Stapleton, and D. J. Tildesley, Molec. Phys. **63,** 527 (1988).
[52] J. VandeVondele, M. Krack, F. Mohamed, M. Parrinello, T. Chassaing, and J. Hutter, Comput. Phys. Comm. **167,** 103 (2005).
[53] G. Lippert, J. Hutter, and M. Parrinello, Molec. Phys. **92,** 477 (1997).
[54] A. D. Becke, Phys. Rev. A **38,** 3098 (1988).
[55] C. Lee, W. Yang, and R. G. Parr, Phys. Rev. B **37,** 785 (1988).
[56] J. P. Perdew, K. Burke, and M. Ernzerhof, Phys. Rev. Lett. **77,** 3865 (1996).
[57] A. D. Boese, J. M. L. Martin, and N. C. Handy, J. Chem. Phys. **119,** 3005 (2003).
[58] S. Goedecker, M. Teter, and J. Hutter, Phys. Rev. B **54,** 1703 (1996).
[59] C. Hartwigsen, S. Goedecker, and J. Hutter, Phys. Rev. B **58,** 3641 (1998).
[60] R. D. King-Smith and D. Vanderbilt, Phys. Rev. B **47,** 1651 (1993).
[61] N. Marzari and D. Vanderbilt, Phys. Rev. B **56,** 12847 (1997).
[62] J. R. Errington and P. G. Debenedetti, Nature **409,** 318 (2001).
[63] Ph. Wernet, D. Nordlund, U. Bergmann, M. Cavalleri, M. Odelius, H. Ogasawara, L. Å. Näslund, T. K. Hirsch, L. Ojamäe, P. Glatzel, L. G. M. Pettersson, and A. Nilsson, Science **304,** 995 (2004).
[64] R. F. W. Bader, *Atoms in Molecules* (Oxford University Press, New York, 1994).
[65] C. J. Cramer, *Essentials of Computational Chemistry* (Wiley, West Sussex, 2002).